On Goodness of WiFi based Monitoring of Sleep Vital Signs in the Wild

Kamran Ali, Mohammed Alloulah, Fahim Kawsar, Alex X. Liu

Abstract—WiFi channel state information (CSI) has emerged as a plausible modality for sensing different human vital signs, i.e. respiration and body motion, as a function of modulated wireless signals that travel between WiFi devices. Although a remarkable proposition, most of the existing research in this space struggles to withstand robust performance beyond experimental conditions. To this end, we take a careful look at the dynamics of WiFi signals under human respiration and body motions in the wild. We first characterize the WiFi signal components—multipath and signal subspace—that are modulated by human respiration and body motions. We extrapolate on a set of transformations, including first-order differentiation, max-min normalization and component projections, that faithfully explains and quantifies the dynamics of respiration and body motions on WiFi signals. Grounded in this characterization, we propose two methods: 1) a respiration tracking technique that models the peak dynamics observed in the time-varying signal subspace and 2) a body-motion tracking technique built with a multi-dimensional clustering of evolving signal subspace. Finally, we reflect on the manifestation of these techniques in a practical sleep monitoring application. Our systematic evaluation with over 550 hours of data from 5 users covering both line-of-sight (LOS) and non-line-of-sight (NLOS) settings shows that the proposed techniques can achieve comparable performance to purpose-built pulse-Doppler radar.

Index Terms—WiFi Sensing, Channel State Information, Sleep Monitoring, Real-World Evaluation

1 Introduction

Respiration rate and body motions are critical indicators of an individual's general state of health. They carry meaningful insights to assess different cardiovascular, neurological, and psychiatric functions of the human body and play an essential role in early diagnosis of various medical conditions, including sleep apnea, asthma, nausea, and several others. Most of the technologies that can monitor respiration and body motions simultaneously are invasive and require the subject to be connected to the measuring equipment, e.g., a respiratory inductance plethysmography belt or multiple wearable sensors. While these instruments certainly offer medical-grade insights, they are not suitable for long-term usage due to their poor ergonomics that hinder long-term assessment. Several other less obtrusive methods have been proposed for tracking vital signs, for instance, Actigraphy [1], [2], [3], [4], [5], [6], [7] and EEG [8] based techniques. However, these methods still require body contact, which is something people are often not comfortable with [9].

Naturally, contact-less vital signs monitoring technologies have attracted significant interest, which mainly include Audio [10], [11], [12], Video [13], [14], Bed sensors (*e.g.* Ballistocardiography (BCG), pressure and/or motion sensors based techniques) [15], [16], [17], [18], [19], [20] and RF sensing based techniques - e.g., mmWave, Frequency Modulated Continuous Wave (FMCW) radar, Pulse-Doppler radar, RFIDs and WiFi based techniques [21], [22], [23], [24], [25], [26], [27], [28]. RF-based techniques are by far some of the least intrusive methods, both in terms of privacy and convenience of use. Radar-based techniques can monitor breathing and other movements reasonably well, however, their operation often requires line-of-sight (LOS) which leads to deployment complexity and significant directivity issues. In contrast, WiFi, and in particular channel state information (CSI) signals of WiFi have emerged as an attractive modality to track respiration and body motions [29], [23], [22], [30], [31]. The fundamental principle of these works is to model the variation of wireless signals modulated by the respiration and motion of a human body. These works have shown the remarkable ability to repurpose WiFi signals to track vital signs; however, unfortunately, often under constrained and controlled settings with strict assumptions. For example, the techniques proposed in existing works have been designed based on controlled experiments often performed on the same subject, where they require the subject to lie down in between or very close to both transmitter (Tx) and the receiver (Rx) to ensure line-of-sight (LOS) scenarios. Their techniques rely on trial-and-error based positioning of WiFi transceivers and signal processing methods to track vital signs, which often leads to high dependency on multiple, environment-dependent parameters that are difficult to tune in real life. Such techniques may be suitable for controlled short-duration lab experiments. However, their suitability cannot be generalized to different individuals, environments, positioning of WiFi transceivers, LOS/NLOS situations, and to natural in-home monitoring scenarios.

Building on the existing WiFi based vital signs monitor-

- *K. Ali is with General Motors Research & Development, Warren, MI, 48557, USA. Email: kamran.lumininte@gmail.com.*
- *M. Alloulah is with the Nokia Bell Labs, USA. E-mail: alloulah@outlook.com*
- *F. Kawsar is with the Nokia Bell Labs, Cambridge, UK. E-mail: fahim.kawsar@nokia-bell-labs.com*
- *Alex X. Liu is with Qilu University of Technology, Changqing District, Jinan, Shandong, China. Email: alexliu360@gmail.com.*
- *Kamran Ali did a part of this work during his internship at Nokia Bell Labs and completed it during his PhD at Michigan State University, USA.*

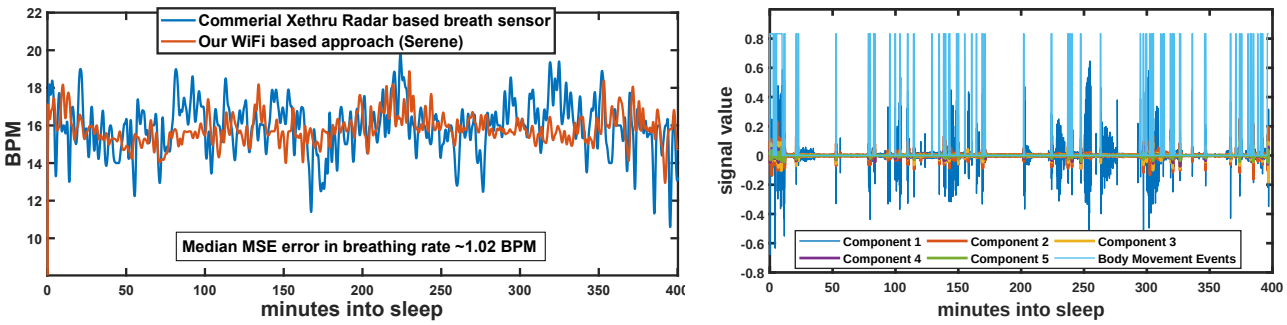

(a) Respiration tracking (full night's sleep)

(b) Body movement tracking (full night's sleep)

Fig. 1: Example showing our system tracking breathing and body movements throughout full night's sleep of subject.

ing works and recognizing their aforementioned limitations, in this work, we take a close look at the dynamics of WiFi, human respiration, and body motions in the wild. Extrapolating on a set of transformations including first-order differentiation, min-max normalization and component projections, first, we analyze the impact of respiration on the multipath components of WiFi signal to quantify the effect of small breathing movements on the CSI signals. Second, we analyze the impact of respiration on WiFi signals subspace to quantify how breathing affects the spatio-frequency subspace—formed by multiple Tx-Rx antennas (MIMO) and Orthogonal Frequency Division Multiplexing (OFDM) subcarriers—very differently compared to other bodily motions (such as slight head or limb movements). Collectively, these characterizations enable us to develop two robust methods for tracking respiration and body motions without any constrains. Moreover, these techniques eliminate user- and environment-specific calibration efforts and as such, allow us to build a system that can track vital signs using design-time training data obtained from only a few configurations and users.

We systematically evaluate our methods by first taking sleep monitoring as a case study, where we collected more than 550 hours (80 nights) of data from 5 users at their respective apartments in real-world full-night sleep monitoring settings. Our experiments covered both line-of-sight (LOS) and non-line-of-sight (NLOS) scenarios such that 55% of our dataset corresponds to NLOS deployment scenarios, and 45% to LOS. Second, we develop a system named *Serene* that implements our proposed methods to track vital signs during sleep. We evaluate Serene's performance in terms of *breath rate error*, number of *motion false positives* that occur in a user's environment (e.g. due to activities of other house residents while the user is sleeping), and *breath signal outage* during which Serene cannot track a subject's vital signs but the ground truth device can. Our results demonstrate that the proposed techniques were able to track respiration rate with an average error of $<$1.19 breaths per minute (BPM). The breath rate error varied between 0.34 BPM to more than 5 BPM depending upon the time of night as a user's sleep posture and distance from the sleep monitor can change during sleep. Figures 1(a) and 1(b) show how Serene tracks breathing and body movement during a full night's sleep of a subject, when the WiFi sleep monitor was placed on a table close to the subject's bed and the router was placed in their TV lounge.

2 Understanding The Relationship between Vital Signs and WiFi CSI

2.1 Overview of WiFi CSI

WiFi devices measure the Channel State Information (CSI), which characterises the surrounding wireless channel across bandwidth and multiple antennae. The Orthogonal Frequency Division Multiplexing (OFDM) communication scheme used in IEEE 802.11a/n/ac divides the wireless channel bandwidth into multiple modulated subcarriers. To correct for channel frequency-selectivity (or equivalently the *delayspread* in time-domain) and maximise the link's capacity, WiFi devices continuously track changes over these subcarriers in terms of CSI values, which are then used to adapt transmission power and rates in real-time. CSI values are the *Channel Frequency Response* (CFR) at per subcarrier granularity between each transmit-receive (Tx-Rx) antenna pair. When a user is breathing, the chest and body movements change the constructive and destructive interference patterns of the WiFi signals. The CSI values are sensitive enough to measure these breathing movements, as CSI measurements can be obtained at high sampling rates and from multiple different OFDM subcarriers of each Tx-Rx stream. For example, the driver of the Intel 5300 WiFi NIC, which we use to implement our scheme, reports CSI values on 30 OFDM subcarriers [32] for each Tx-Rx antenna pair for every CSI measurement. This leads to 30 matrices with dimensions $M_t \times M_r$ per CSI sample, where M_t and M_r denote the number of transmit and receive antennas respectively. Such high dimensional data allows us to recover detailed information about the vital signs even if the breathing and body/limb related movements only incur small changes in the CSI.

2.2 Impact of Breathing on WiFi Multipath

Next, we present our first analysis that is aimed at understanding the effect of small breathing movements on the WiFi multipath and CSI signals. Based on this analysis, we design Serene's signal processing pipeline to robustly extract breathing waveforms in an individual and environment independent manner. Our analysis shows that if we differentiate (*i.e.* by taking *first order difference*) the CSI signals from each WiFi subcarrier, and then *max-min normalize* the CSI signal projection corresponding to variations due to breathing, we can robustly extract the waveform corresponding to a user's breathing motion in an environment and individual independent manner, as long as the user sleeps close to the WiFi receiver. Such proximity

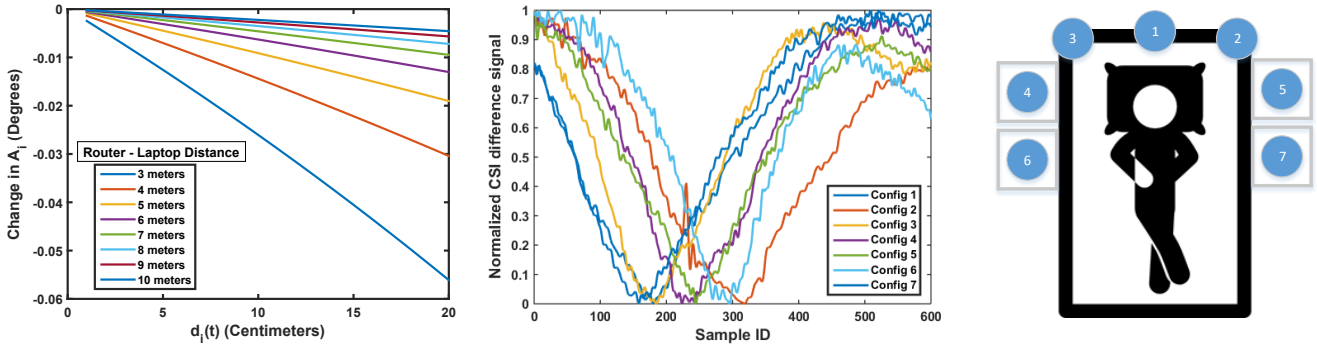

(a) Variation of A_i with $d_i(t)$ for $D_{0,i}$ 3 to 10 (b) Single breath samples for 7 configurations (c) Configurations of receiver

Fig. 2: (a) Variation of A_i with $d_i(t)$ for different $D_{0,i}$; (b) Single breath samples for different configurations in (c)

requirement is easy to satisfy during real-life in-home sleep scenarios by either mounting the receiver on the headboard of a bed frame or placing it on a table nearby. *Note that differentiation generally degrades signal-to-noise ratio, unless the differentiation algorithm includes smoothing that is carefully optimized for the application at hand. Therefore, we introduce a combination of low-pass filters (i.e. median, exponential moving average, and Butterworth filters (§3.1)) in Serene's signal processing pipeline. We experimentally design these filters such that signal-to-noise ratio is sufficiently good for a reasonable quantitative measurement of the sleep related vital signs. The max-min normalization is performed after the filtering process to estimate the breath rate (§3.3.2).* At the basis of our analysis is a closed form expression, which we derive using time-varying Channel Frequency Response (CFR) of WiFi channel. The time-varying CFR corresponding to a Tx-Rx antenna pair for a subcarrier with wavelength λ can be quantified as:

$$H(f,t) = H_s(f) + \underbrace{\sum_{i=1}^{N} \frac{K}{D_i(t)^2} e^{\frac{j2\pi D_i(t)}{\lambda}}}_{H_d(f,t)} \quad (1)$$

In the equation above, N is the number of multipath reflections of the transmitted signal at the Rx end, D_i represents the distance traveled by i^{th} multipath reflection, and K is an environment dependent proportionality constant. $H_s(f)$ is the *static* component of CFR corresponding to all non-user multipath reflections (i.e. the CFR when there is no interference due to other networks or movement in the environment), while the second term on the right hand side corresponds to the *dynamic* component of CFR, represented as $H_d(f,t)$, while the user is breathing and/or moving during sleeping. Moreover, in the context of sleep monitoring, when we say $H_s(f)$ is "static", we mean that it is static in the short-term. The changes and/or interferences that are dynamic in the short-term (such as the ones caused by fans, interfering wireless networks, movement of other persons in the room, etc.) are captured by the dynamic component of CFR $H_d(f,t)$. However, $H_s(f)$ can change in the long-term, for example, due to environmental changes such as addition of a new piece of furniture in a room or addition of new person in the room or even when the sleeping person changes their posture (because after a change in sleep posture, the positions of different body parts that reflect WiFi signals also change). That is why, we continuously perform differential sensing, which reduces the impact of such longer-term changes in $H_s(f)$. Now, let us assume that user is sleeping at a distance $D_{0,i}$ from the router, and $d_i(t)$ is the change in distance traveled by i^{th} reflected path due to breathing. To make our scheme resistant to static changes in the environment, we first eliminate $H_s(f)$ by differentiating the above equation with respect to t, and substitute $D_i(t) = D_{0,i} + d_i(t)$ to get:

$$H'(f,t) = \frac{d}{dt}\left[\sum_{i=1}^{N} \frac{k}{D_{0,i}^2}\left(1 + \frac{d_i(t)}{D_{0,i}}\right)^{-2} e^{\frac{j2\pi(D_{0,i}+d_i(t))}{\lambda}}\right] \quad (2)$$

As $d_i(t)$ caused by motion due to breathing is in the order of a few centimeters, whereas $D_{0,i}$ is usually in the order of meters (i.e. $d_i(t) \ll D_{0,i}$), we can expand the negative polynomial $(1 + \frac{d_i(t)}{D_{0,i}})^{-2}$ via binomial series expansion. After performing binomial expansion, discarding the $\frac{d_i(t)^m}{(D_{0,i})^n}$ terms with n = 4 or higher, and doing some algebraic manipulations, we get the following expression for $H'(f,t)$:

$$H' \approx ke^{\frac{j2\pi D_{0,i}}{\lambda}} \times \left[\sum_{i=1}^{N} d_i'(t)\left(-\frac{2}{D_{0,i}^3} + j\left(\frac{2\pi}{\lambda D_{0,i}^2} - \frac{4\pi d_i(t)}{\lambda D_{0,i}^3}\right)\right) e^{\frac{j2\pi d_i(t)}{\lambda}}\right]$$

After converting the term inside summation into polar coordinates, and discarding the $\frac{d_i(t)^m}{(D_{0,i})^n}$ terms with n = 4 or higher, we get the following simplified expression for $H'(f,t)$:

$$H' \approx \left[\frac{2\pi k}{\lambda D_{0,i}^2}\sqrt{1 + \left(\frac{\lambda}{\pi D_{0,i}}\right)^2} \times e^{\frac{j2\pi D_{0,i}}{\lambda}}\right] \cdot \left[\sum_{i=1}^{N} d_i'(t) e^{\frac{j2\pi d_i(t)}{\lambda} + jA_i}\right]$$

Here, $A_i = tan^{-1}\left[\frac{\pi D_{0,i}}{\lambda}\left(1 - \frac{2 \cdot d_i(t)}{D_{0,i}}\right)\right]$. Figure 2(a) shows variation of A_i with $d_i(t)$, as $d_i(t)$ varies from 1cm to 20cm (typical range for motion due to human breathing is 1-5cm [33]), for different router-receiver distances $D_{0,i}$ ranging from 3m - 10m (*i.e.* which is typical for in-home use cases).

We observe that changes in $d_i(t)$ do not significantly affect the value of A_i. Moreover, the impact of $d_i(t)$ on A_i

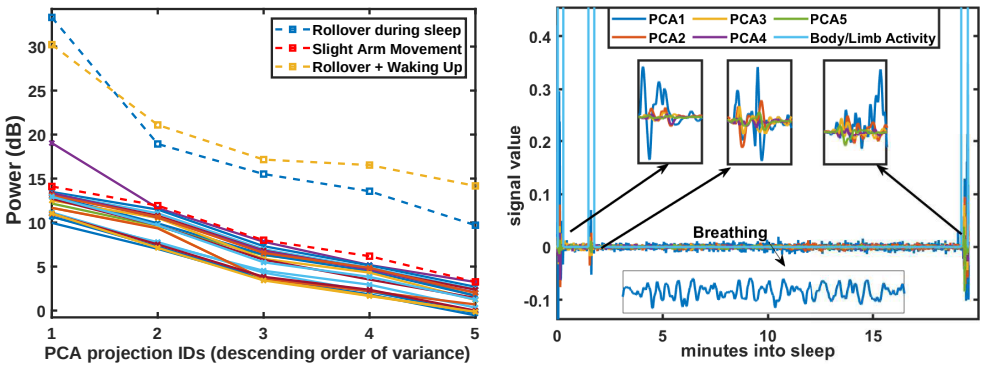

(a) Power values in top PCA projections

(b) CSI timeseries for Fig. 3(a)

Fig. 3: Impact of bodily activity during sleep on WiFi subspace

decreases even further as the distance between receiver and the router it is connected to increases. Therefore, we can safely approximate $A_i \approx tan^{-1}\left[\frac{\pi D_{0,i}}{\lambda}\right] = A_{0,i}$ and write $H'(f,t)$ as:

$$H' \approx \left[\left(\frac{2\pi k}{\lambda D_{0,i}^2}\sqrt{1+\left(\frac{\lambda}{\pi D_{0,i}}\right)^2}\right)\times e^{j\left(\frac{2\pi D_{0,i}}{\lambda}+A_{0,i}\right)}\right] \times \sum_{i=1}^{N} d_i'(t)e^{\frac{j2\pi d_i(t)}{\lambda}}$$

The first term on right hand side of the equation above stays constant when receiver is placed on some surface, *e.g.* a desk/table, and is not moving. We write amplitude of CFR *i.e.* $|H'(f,t)|$ as:

$$|H'(f,t)| \approx C_{0,i} \cdot \left|\sum_{i=1}^{N} d_i'(t)e^{\frac{j2\pi d_i(t)}{\lambda}}\right| \quad (3)$$

The waveform $\left|\sum_{i=1}^{N} d_i'(t)e^{\frac{j2\pi d_i(t)}{\lambda}}\right|$ corresponds to the variations due to breathing. The proportionality term $C_{0,i}$ in breathing samples extracted from $|H'(f,t)|$ corresponding to different placement of receiver can be easily eliminated via *max-min normalization*. Figure 2(b) shows extracted and processed single breath samples from a user for seven slightly different receiver placement configurations close to the user, while the router was in a subject's TV-lounge (router-receiver distance >10 meters).

2.3 Impact of Breathing and Body/Limb Movements on WiFi Signal Subspace

Next, we present our second analysis that is aimed to understand how breathing affects the signal subspace formed by WiFi subcarriers compared to other bodily movements. Today's MIMO and OFDM based WiFi devices use many frequency subcarriers and multiple transmit-receive (Tx-Rx) antennas for data communication. The MIMO system between the OFDM subcarriers and the Tx-Rx antennas, forms a multidimensional array which effectively represents a high-dimensional mathematical space. Contained in this space is the signal subspace along frequency and spatial dimensions [34]. The key intuition behind our model is that while a user is sleeping, the signal subspace along these dimensions is affected by both breathing and body/limb motion. When there is no body/limb motion, there is only one dominant time-varying component in the subspace, which corresponds to breathing. However, more components along these dimensions evolve (*i.e.* show considerable variations) during other body/limb activity *e.g.* during roll overs or arm/leg movement. Based on this principle, Serene isolates breathing from limb motion without requiring any environment-dependent calibrations.

To model this in Serene, we track the top dominant components in the CSI signal subspace using Principal Component Analysis (PCA). Figure 3(a) shows power values in top 5 PCA projections of the CSI signals corresponding to multiple sleep epochs during a sleep experiment, where the dotted lines correspond to epochs with motion events—highlighted in Figure 3(b). We observe that in the absence of any body/limb activity, the top-most PCA projection is enough to track breathing as it is the only major motion occurring in the environment. However, during body/limb movements, multiple lower PCA projections also show significant variations. Based on this phenomenon, we accurately detect and then discard the CSI values corresponding to any body/limb activity by tracking variations in the lower PCA components (*e.g.* 3, 4 and 5) using a multi-dimensional clustering technique, which we discuss in §3.2. *Note that although PCA based approaches have been used in the previous CSI-based sensing works, yet ours is the first work to study, characterize, and build on the "intra-subspace" dynamics of WiFi signals [34] for respiration and body motions.*

3 CSI Signal Processing Architecture

To obtain CSI data in real-time during sleep, we develop a client-server based mechanism to communicate the CSI values extracted from WiFi NIC to a Python based CSI processing server. Based on our discussion in §2, we take first order difference of the incoming CSI data and then take its amplitude *i.e.* $|H'(f,t)|$ for further processing. From now onward, we use the term "CSI" to denote $|H'(f,t)|$. CSI data is collected in 30 second epochs, which is typically the partitioning convention followed by most sleep monitoring systems. Next, we first perform basic low-pass filtering for removing bursty noise due to hardware noise and isolate the signal of interest i.e. to extract human motion related frequencies only. Second, we perform PCA on the low-pass filtered CSI streams for dimensionality reduction and automatic distinguishing of CSI variations due to body movements from those of breathing in different

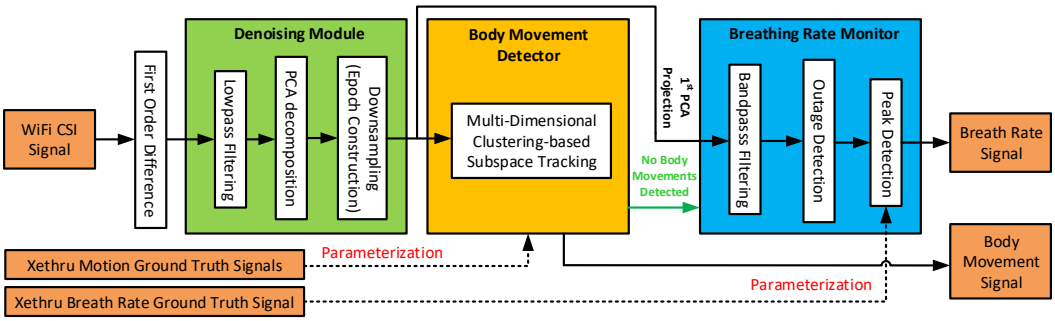

Fig. 4: Our WiFi CSI signal processing architecture for extracting vital signs

subcarriers based on our discussion in §2.3. This avoids the need for complex trial-and-error based subcarrier selection procedures used in previous works [23], [22]. Third, we harmonise the filtered CSI data corresponding to each 30s sleep epoch into uniformly sampled and consistent measurements via down-sampling. Fourth, we robustly detect body movements by tracking lower PCA projections of CSI signals using a clustering-based event detection technique. Finally, we first detect the presence of breathing using a power threshold, and then perform further band-pass filtering to extract the signal corresponding to breathing. Figure 4 shows our system architecture. Next, we briefly discuss Serene's noise removal process.

3.1 Noise Removal

Commodity Wi-Fi NICs report noisy CSI values, both due to hardware limitations (such as low resolution Analog to Digital Converters (ADCs)) and due to changing transmission power and rates. We use a combination of median filter and an exponential moving average filter to get rid of such bursty noise and spikes in CSI time series. After this basic filtering step, we further remove any high frequency variations in CSI signals using *Butterworth* low-pass filter. Variations due to movement during sleep cause low frequency variations, typically under 5 Hz [33]. We use Butterworth low-pass filter for separating these variations from higher frequency noise in CSI values. Due to maximally flat amplitude response of Butterworth filter, its application on CSI time series does not distort the shape of CSI variations due to body motion. Our scheme samples CSI values at a nominal frequency $F_s = 800$. With this in mind, we use cut-off frequency $\omega_c = \frac{2\pi * f}{F_s} = 0.0125\pi$ rad/s for Butterworth filtering. We apply the same filter on CSI timeseries of all the subcarriers, making sure that every CSI stream experiences the same phase distortion and group delay introduced by the filter.

Based on our experimental results, we observed that filtered CSI waveforms still retain some noisy variations which are not related to activity/breathing. We avoid any further low pass filtering on CSI streams as it can lead to loss in details of variations due to activity/breathing behavior. To remove such noise, we utilize the fact that the CSI variations in CSI streams of multiple subcarriers in each Tx-Rx antenna pair are correlated. We apply PCA on CSI obtained from all subcarriers and all Tx-Rx pairs, and retain only the waveforms that represent the most common variations in all the subcarriers, i.e., the variations due to breathing and/or body movements during sleep. That is, signal subspace-based filtering enables our scheme to automatically obtain the signals that are representative of the monitored vital signs only. Finally, we rearrange the multi-dimensional filtered CSI data corresponding to each 30s sleep epoch into consistent length samples (600 in our current implementation) via down-sampling, performing zero-padding where necessary. We concatenate data from consecutive epochs for real-time tracking of vital signs (*e.g.* breathing) which we discuss later in this section.

3.2 Tracking Body Movements

We observed that when there is no body/limb motion, there is only one dominant, time-varying component in the signal subspace, which corresponds to breathing. PCA sorts different principal components in descending order of their variation. During sleep, the signal subspace is rather quiet and breath is captured in the top PCA projection of the CSI time series. However, we observed that during episodes of other body movements—*e.g.* during roll overs or arm/leg movement—more signal subspace components evolve, since body movements cause more pronounced variations in the spatial-frequency subspace compared to faint breathing movements.

3.2.1 Body Movements Detection Approach

To robustly distinguish body activity/limb motion from breathing, we propose to use a multi-dimensional *hyper-ellipsoidal* clustering on the lower PCA projections of CSI data. At a high-level, we can think of this clustering method as a high-dimensional generalization to a Gaussian outlier rejection technique whereby measurements few sigma's away from the mean are deemed erroneous. Specifically, let $R_k = \{r_1, r_2, \cdots r_k\}$ be the first k samples of CSI vectors containing values from the selected signal subspace—*we use PCA projections 3, 4 and 5 in our current implementation*. Each sample r_i is a $d \times 1$ vector in $\mathbb{R}^d$, where d is the number of signal subspace components. This *hyper-ellipsoidal* technique clusters the normal data points (i.e. when there is no body movement in the environment), and any points lying outside the cluster are declared as outliers. The boundary of the cluster (a "hyper-ellipsoid" in this case) is related to a distance metric which is a function of mean $m_{R,k}$ and covariance S_k of the incoming signal subspace components R_k. We use the *Mahalanobis* distance metric, D_i, for which the cluster is arrived at according to the following [35]:

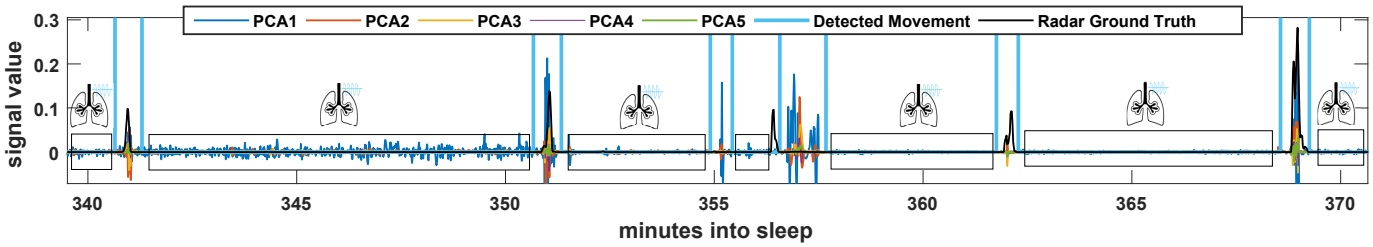

Fig. 5: Example showing performance of our body movement detection algorithm, compared to Xethru ground truth. Boxes show the areas where breathing is usually present. Ground truth is approximately synchronized with CSI data.

$$e_k(m_R, S_k^{-1}, t) = \{r_i \epsilon \mathbb{R}^d | \underbrace{\sqrt{(r_i - m_{R,k})^T {S_k}^{-1} (r_i - m_{R,k})}}_{D_i = Mahalanobis \;\; distance \;\; of \;\; r_i} \leq t\} \tag{4}$$

where e_k is the set of normal data points whose Mahalanobis distance, $D_i < t$ and t is the *effective* radius of the hyper-ellipsoid. The choice of t depends on the distribution of the normal data points. If the normal data follows a *chi-squared* distribution, it has been shown that up to 98% of the incoming normal data can be enclosed by the boundary of an hyper-ellipsoid, if the effective radius t is chosen such that $t^2 = (\chi_d{}^2)^{-1}_{0.98}$ [35]. Data samples r_i for which $D_i > t$, are therefore, identified as outliers. As it is often not practical to store all the samples of a streaming data, a recursive algorithm is required to update e_k. Let r_{k+1} be the most recent CSI sample. $m_{R,k+1} = \frac{k m_{R,k} + r_{k+1}}{k+1}$ and $m_{R^2,k+1} = \frac{k m_{R^2,k} + r_{k+1} r_{k+1}^T}{k+1}$ can be updated recursively from the previous means. By substituting covariance matrix $S_k = m_{R^2,k} - (m_{R,k}\, m_{R,k}^T)$ into Eq. (4) we can represent e_k entirely in terms of means. The resulting equation updates the cluster boundary and classifies the incoming data samples as normal readings or outliers. Our scheme uses above equations for initial estimation of mean and covariance. Afterwards, the mean $m_{R,k}$ is recursively calculated using an exponential moving average technique, where mean $m_{R,k+1}$ is updated as $m_{R,k+1} = \alpha\; m_{R,k} + (1-\alpha) r_{k+1}$, where $\alpha = 0.9995$ in our implementation. Moreover, after initial estimation of covariance, our scheme recursively updates the covariance inverse S_k^{-1} by using the following equation [35], which avoids extra computations required for calculating the inverse of matrix S:

$$S_{k+1}^{-1} = \frac{k S_k^{-1}}{\alpha(k-1)} \times \left[I - \frac{(r_{k+1} - m_{R,k})(r_{k+1} - m_{R,k})^T S_k^{-1}}{\frac{(k-1)}{\alpha} + (r_{k+1} - m_{R,k})^T S_k^{-1} (r_{k+1} - m_{R,k})} \right] \tag{5}$$

To determine the start and end of activity waveforms, we use both cardinality and temporal proximity of the detected outliers. If the number of consecutive outliers increases a threshold E_1, we declare a micro-event. Multiple micro-events constitute a activity event. All the data points including the points constituting the micro-events as well as the points in between the consecutive micro-events are recorded as part of activity waveform (*merging*). We only merge the micro-events which are within E_2 data points of each other. Both E1 and E2 are design-time, easy to tune thresholds. Figure 5 shows some body movements detected by our algorithm in a portion of processed CSI timeseries corresponding to an in-home full-night sleep monitoring experiment.

3.3 Tracking Breath

Human breath involves motion of chest and lungs during inspiration (when air enters the lungs) and expiration (when air is blown out from the lungs) [33]. These motions are often periodic (e.g. in case of healthy subjects [33]), and therefore, cause periodic variations in WiFi channel which we can extract using CSI data. In the absence other body movements, the first PCA projection of CSI data would be able to capture these variations due to breathing. However, as these minute variations are often embedded in noise, and because human subject might not be in proximity of the Rx device, we can not always assume that breathing signal exists in a particular sleep epoch. Therefore, to robustly track breathing, we propose the following signal processing pipeline.

3.3.1 Bandpass Filtering

To extract the periodic variations in CSI due to breathing, we apply a Butterworth bandpass filter on the first PCA projection. We choose the filtering parameters of this filter according to the fact that breathing rate of humans (including adults as well as newly born babies) ranges between 10 - 40 breaths per minute (BPM) [33]. This step removes any non-breathing related noise present in the signal.

3.3.2 Measuring Breathing Rate

We design our system to measure breathing rate in terms of breaths per minute (BPM). We measure the rate over a window of two sleep epochs in length, which moves over concatenated data from multiple consecutive sleep epochs. To report BPM every second, we move this window over the concatenated data every second (i.e. 20 samples a time).

To measure breathing rate, we employ a *peak detection* based approach. First, we max-min normalize the signal so that parametrization of our peak detection algorithm can be easily generalized to different users. Second, to robustly detect the number of peaks, we use three parameters, namely *minimum peak prominence* (MINPRO), *minimum peak distance* (MINDIST), and *minimum peak strength* (MINSTR). The prominence of a peak measures how much the peak stands out, due to its height and location, relative to other peaks around it. We tune MINPRO such that we only detect those peaks which have a relative importance of at least MINPRO. We tune MINDIST according to the fact that human breathing rate ranges between 10-40 BPM [33],

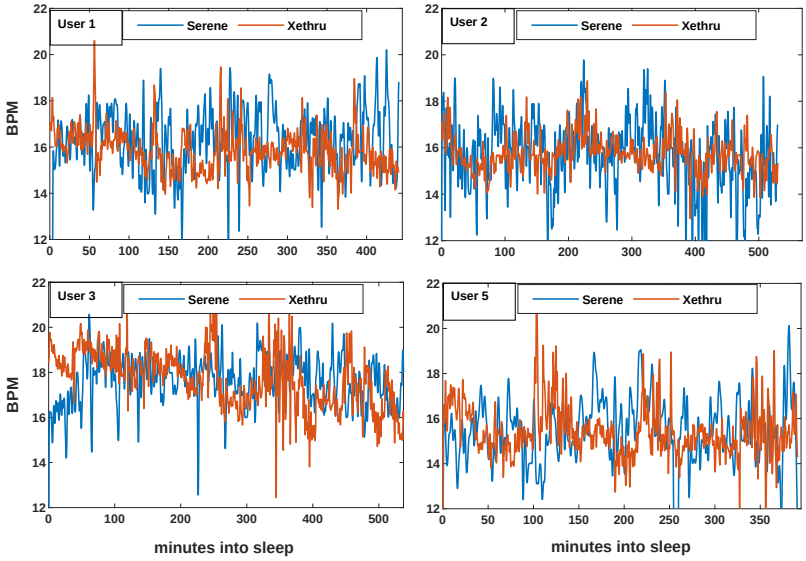

Fig. 6: Full-night breath tracking examples.

so that redundant peaks are discarded. To further sift out redundant peaks, we only choose peaks of value greater than MINSTR times the median peak value. In our current implementation, we chose MINPRO = 0.025, MINDIST = 1.5 seconds and MINSTR = 0.6 which generalize well for different sleeping scenarios. *To achieve accurate tracking of breathing rate, we perform parameterization of Serene's breath estimation algorithm using ground truths obtained from a contact-less COTS Xethru X4M200 Breath/Motion sensor [36]. We perform this parametrization only during the design of our system and do not require any end-user calibration effort in real-world deployments.*

4 Implementation and Evaluation

Fig. 7: The real-world deployment scenarios used for evaluation of Serene.

4.1 Hardware Implementation

We developed compact HummingBoard (HMB)-based small-sized nodes as sleep monitoring devices [37] which makes Serene easy to deploy. HMB nodes were equipped with the Intel 5300 NICs with modified drivers for extracting CSI information [32]. We used Linksys AC1200+ routers as transmitters in our deployments. Moreover, we developed a client-server software architecture—in C and Python respectively—capable of the real-time extraction and processing of CSI data throughout the night. For body movement and breathing rate ground truths, we deployed state-of-the-art *pulse-doppler* radar-based Xethru X4M200 Breath/Motion sensors [36]. In terms of breathing rate accuracy, the X4M200 devices have been shown to perform very closely to a medical-grade, gold standard equipment (X4M200 has been shown to track breathing with up to 96% accuracy when compared to PSG) [38]. We chose a contactless sensor to record ground truths because the participants of our study were not comfortable wearing devices such as breath monitoring belts during their regular sleep. Moreover, the devices that require body contact generally tend to interfere with natural sleep of the users [9].

4.2 Experimental Settings

We deployed our system in 5 apartments, where we collectively recorded more than 80 nights (>550 hours) of data from 5 different participants. Each of the 5 participants of our study lived in different apartments and every apartment was tested with the occupant of that apartment only. The participants were graduate students aged between 23 to 32 years. The duration of data collection for each participant varied from 5 to 31 days. Figure 7 shows the real-world deployment scenarios for our sleep experiments. The numbers in circles specify user/environment IDs. Data collected from environments 2 and 3 corresponds to NLOS deployment scenario, and constitutes 55% of our dataset. Data collected from environments 1, 4, and 5 corresponds to LOS deployment scenario, and constitutes 45% of our dataset. To evaluate Serene's vital signs tracking performance, we collected Xethru ground truth alongside CSI data for the environments 1, 2, 3 and 5. We evaluate Serene's performance in terms of three key metrics: (1) breath tracking accuracy, (2) breathing signal outage (during which Serene cannot track breathing), and (3) naturally occurring motion false positives due to activities of other house occupants. Overall, we were able to collect 15, 31, 14, 16, and 5 nights of data from users 1, 2, 3, 4, and 5, respectively.

4.3 Breath Tracking Accuracy

We evaluate the accuracy of Serene's breathing rate estimation in terms of *BPM error*. We define BPM error as the average mean squared error (MSE) between per second BPM

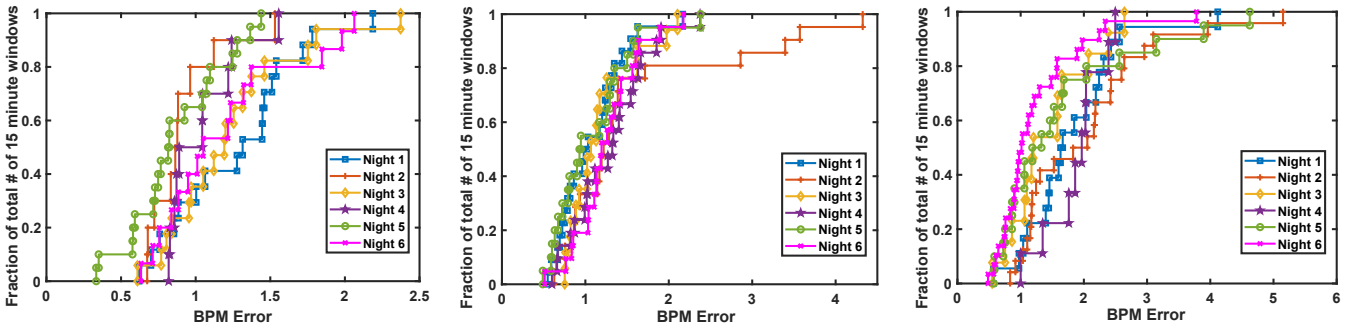

(a) User 1, 6 nights. (b) User 2, 6 nights. (c) User 3, 6 nights.

Fig. 8: CDFs of BPM errors calculated over 15 minute windows for 6 different nights (Users 1, 2 and 3).

values reported by Serene and the corresponding ground truth BPM values reported by X4M200 over a specific time window. We perform this evaluation on data collected from environments 1,2,3 and 5. Due to deployment issues, we could not collect ground-truth data from environment 4 for a meaningful analysis required for this subsection. Therefore, we exclude that user's data from the following discussion. We evaluate both long-term (*i.e.* whole night) and short-term (*i.e.* specific short duration sleep windows during the night).

4.3.1 Long-term Accuracy

Serene achieves a median error of less than 1.19 BPM for real-world in-home full night sleep experiments. To evaluate Serene's long-term breath tracking accuracy, we compute the mean squared error (MSE) of instantaneous (per second) breathing rate estimate across an entire night of sleep. The overall cumulative distribution function (CDF) of the MSE error in breath per minute (BPM) is depicted in figure 9(a). Inspecting the blue curve, we see that the median accuracy of Serene's breathing rate estimate is 1.19 BPM, while its 95th percentile confidence is under 1.9 BPM. We skip User 5 CDF from the graph as we were only able to collect 5 nights of data from that user. The average, minimum and maximum BPM errors observed for User 5 were 1.1, 0.811, and 1.14, respectively. Figure 6 shows how Serene tracks breathing rate throughout a night for 4 different users, where we have plotted X4M200 ground truth side by side. We can observe that BPM accuracies vary during the night as a user's sleep posture and distance from the sleep monitor can change during sleep. The sleep posture and distance of a user from the sleep monitoring devices determine how well both X4M200 and WiFi devices can track breathing. Overall, X4M200 experiences negligible outage compared to WiFi, because X4M200 uses a radar signal that uses orders of magnitude more bandwidth and is specifically designed to track respiration and other body movements during sleep (shown to be up to 96% accurate compared to PSG - the gold standard of sleep monitoring). As WiFi can experience significant outage depending upon subjects position from the WiFi receiver or their sleep postures (as discussed later in §4.5), its breath graph can diverge from X4M200's ground truth at different times during a nights sleep. That said, under the right circumstances occurring for some sleep intervals, they can match up very closely. Moreover, we also observe that during some parts of a full-nights sleep, Serene is able to track the overall increasing and decreasing trend in a subject's breath during sleep fairly well when compared to Xethru's ground truth. We discuss some results related to such dynamics later in §4.3.2.

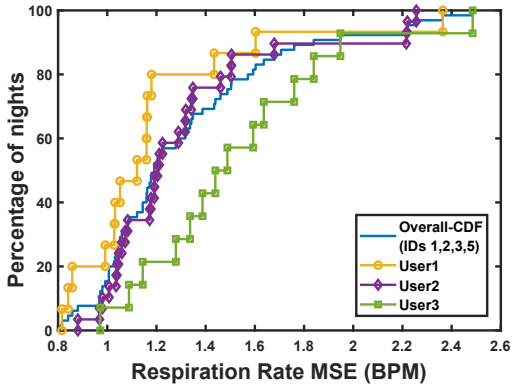

(a) CDF of overall and per-user BPM error.

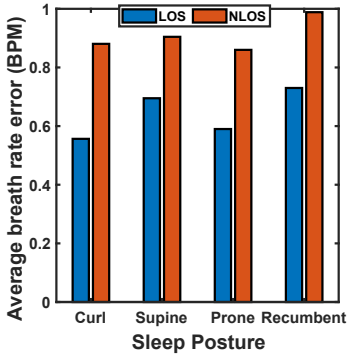

(b) Sleep posture experiments.

Fig. 9: CDF of overall and per-user breathing rate MSE compared to a Xethru ground truth; average BPM errors for short duration sleep posture experiments

Figure 9(a) also shows how BPM accuracy varies across subjects. For instance, the median accuracy was better than 1.12 BPM and 1.2 BPM for users 1 and 2, respectively. However, user 3's median accuracy was a bit higher (*i.e.* 1.488), while the 95th percentile confidence was as large as 1.95 BPM. These slight variations across different users and environments occur due to differences in physiques, respiratory system morphologies and environmental deployment conditions. For example, environments 2 and 3 both correspond to NLOS scenarios, which leads to relatively lower BPM accuracies. Although the level of robustness and accuracy Serene achieves may not be comparable to contact-

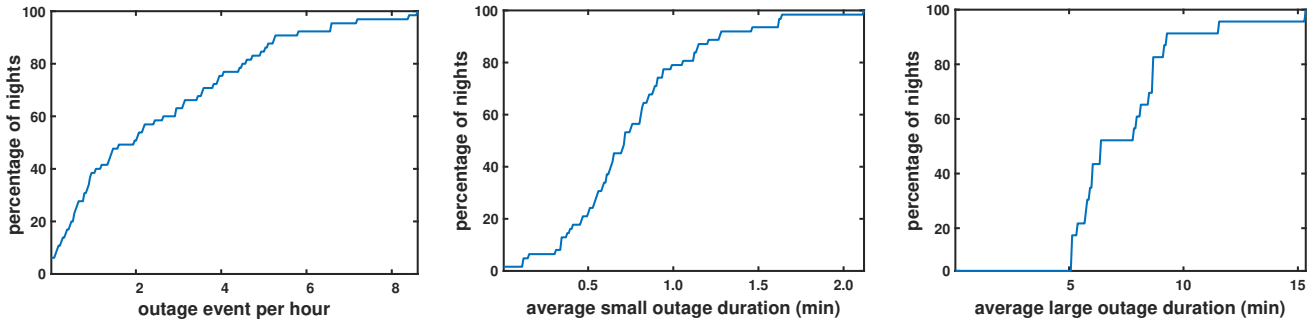

(a) Outage rate (b) small-scale outage duration (c) large-scale outage duration

Fig. 10: Second-order statistics of breath estimation outage events. Outage rate and average outage duration mirror, respectively, their counterparts level crossing rate and average fade duration from wireless propagation literature.

based high accuracy breath monitors, yet it is comparable to other commercial contact-less sleep monitoring products. Therefore, based on our results, we conclude that WiFi based sleep monitors can be robust and accurate enough for daily in-home use to gain insights into overall breathing trends during sleep. However, the accuracy may not be enough for medical grade sleep assessments.

4.3.2 Short-term Accuracy

Serene can achieve an error of as low as 0.34 BPM during certain parts of a full-night sleep. However, the errors can be more than 5 BPM depending upon the time of night as a user's sleep posture and distance from the sleep monitor changes during sleep. In Fig. 6, we notice that there are certain time windows during the night where Serene matches Xethru's performance very closely. To know how many times such time windows occur during different nights in our dataset, we divide each night into small 15 minute time windows and compute the MSE of per second BPM estimate in those windows. Figure 8 show the CDF plots for 6 different full-night sleep experiments corresponding to users 1, 2 and 3. From Fig. 8(a), we observe that in the case of User 1, Serene experienced a breathing rate error of only 0.34 BPM in one 15 minute window during Night 6. Moreover, error in more than 50% of the time windows remained below 0.84 BPM during Night 6. Similarly, for other users, we observe that in multiple time windows during a full-night sleep, BPM error stays under 1 BPM. This shows that Serene does fairly well when compared to controlled short-duration sleep experiments performed in recent CSI based sleep monitoring studies. Also, figure 9(b) shows average BPM errors for controlled 10 minute sleep experiments in different sleep postures. We observe that Serene achieve an error of less than 1 BPM for most sleep postures even in NLOS scenarios. The errors were as low 0.55 BPM in LOS scenarios. However, we also observed errors approaching 5 BPM during certain time windows that can be attributed to changes in the user's sleep posture and distance from the sleep monitor during sleep.

4.4 Naturally Occurring Motion False Positives

Serene experienced a median of 20 false positive limb/body motion events, which can be attributed to activities of other house residents while the user is sleeping. The total duration of such events stayed below 37 minutes more than 95% of the time. Radar and WiFi are both very sensitive to body motion. We observed from our experiments that whenever a user moves in their bed, both Serene and X4M200 successfully detect the motion event. However, we also observed scenarios where Serene detected body movements but the ground truth remained undisturbed (*i.e.* contained breathing signal only). We call such spurious movements detected by Serene as *motion false positives* (MFPs), which we attribute to other movements present in the environment (e.g. when one of the occupants wakes up to get water, etc.). To understand how significant such MFPs can be in real-world deployments of a WiFi based sleep monitor, we evaluate the following two key metrics on the real-life dataset we collected using Serene: (1) the *number* and (2) *duration* of MFPs per night's sleep.

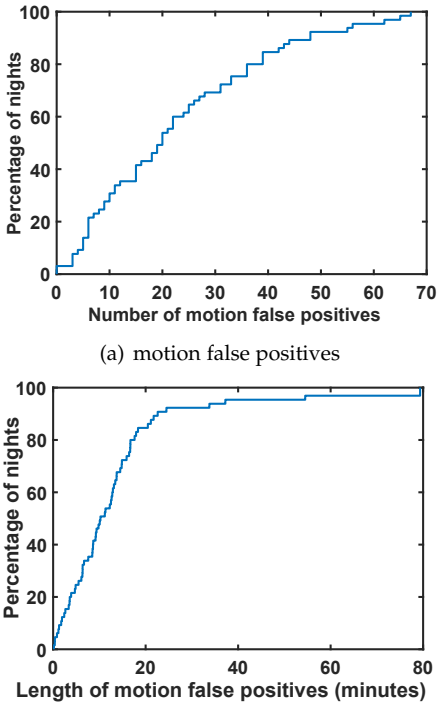

(a) motion false positives

(b) duration of motion false positives

Fig. 11: CDF's of numbers and total duration of motion false positives during a night when compared with X4M200 ground truths. Motion false positives naturally occur due to activities of other housemates.

Figure 11 illustrates the CDFs of these two metrics evaluated over more than 65 nights in our database. We observe that our system detected less than 56 MFPs occurrences for 95% of tested nights 11(a). Moreover, when we observe

that when MFPs occur, their collective duration remains bounded under 37 minutes for 95% of the time, as shown in figure 11(b). Although the total duration of such events during any night's stayed below 10 minutes on average and below 37 minutes 95% of the time, yet we observed motion false positives of more than 60 minutes (1 hour) in total during one of the nights in our dataset. Note that these MFPs do not signify any technical limitation of WiFi based sleep monitoring, as such motions occur naturally in home environments. Our results show that the number and duration of naturally occurring interference in WiFi signals due to activities of other residents is usually low during night time. Therefore, WiFi based sensing is suitable enough to be used for sleep monitoring during night time.

4.5 Breath Signal Outage

4.5.1 Detecting Outage in Breathing Signal

Serene experiences an average outage of less than 6.38 minutes, during which it cannot track any vital signs. We define the *outage* of our system as the event when variations due to breathing are not present in the CSI signal while the ground truth device (i.e. Xethru X4M200 in our case) is able to track breathing.[1] To detect outage, our system first determines the noise floor of the environment using the first PCA projection. During real-time tracking, our system compares the average power of the signal, calculated over 7.5s windows of every 30s sleep epoch (i.e. $1/4^{th}$ of an epoch's duration), with the determined noise floor. If the average power of the sleep epoch is not above the determined noise floor while X4M200 is still able to track breath, Serene signals outage. To assess Serene's ability to continuously track vital signs (*i.e.* breathing and other limb/body activity) in real life, we measure its per-night *outage* performance statistics. To achieve this, we follow the treatment of signal outage in wireless propagation literature. Specifically, we calculate two second-order statistics: level crossing rate (LCR), and average fade duration (AFD) [39]. LCR determines the rate at which outages occur during a full-night sleep, whereas AFD determines the duration of each outage. We analyze the LCR and AFD using the first PCA projection's power with respect to the noise floor.

Figure 10(a) shows LCR or outage rate calculated per hour across our sleep dataset. We can observe that on average, the breathing rate estimation of participants experienced 2 outage events per hour. At 95 percentile confidence, outage amounted to less than 6.6 events per hour. However, in the context of sleep monitoring, a further piece of detail must be considered to fully understand outage events during sleep, *i.e.* the duration of such outages, which we characterize using AFD. Serene can experience two types of outage events: *small-scale* and/or *large-scale*. Such outages arise due to users rolling over in bed to a different position or sleep posture while sleeping. This is because certain sleep postures can make it difficult for Serene to detect the breath signal due to weaker chest movements. To understand how such small-scale and large-scale outage events are distributed naturally in real life, we introduce a design threshold to separate the two types of outage events. From the analysis of our dataset, we set such design threshold to 5 minutes, where we consider outage events longer than 5 minutes as a large-scale outages and vice versa. Figure 10(b) elaborates on the statistical behavior of small-scale outage. On average, small-scale outage events lasted for 0.7 minutes, while the 95th percentile confidence outage duration is under 1.62 minutes. CDF of the duration of large-scale outage is shown in figure 10(c). Large-scale outage duration averaged around 6.38 minutes while its 95th percentile confidence is under 11.56 minutes, although durations in excess of 15 minutes can occur. Based on this analysis, we can conclude that WiFi based sleep monitors experience more outages compared to radar based monitors such as Xethru X4M200. However, we must mention that while collecting the dataset we suggested our subjects not to change the position of X4M200 so that their chest stays in X4M200's line-of-sight. In real life scenarios, users can make mistakes while positioning such radar based sensors before going to sleep which may cause outages similar to the ones experienced by Serene.

1. To detect outage, we use the "absent"'' signal that Xethru X4M200 provides when it cannot detect any motion in the environment.

5 Discussions

Serene is an early step towards characterizing WiFi multipath and signal subspace to faithfully explain and quantify the dynamics of respiration and body motions on WiFi signals. There is obviously room for continued research in various perspectives. In this section, we discuss WiFi based sleep scoring, provide commentary on the limitations of our work, and point to possible avenues of future research.

Sleep Scoring. To motivate the merits of WiFi based sleep monitoring, we present a few interesting insights on sleep quality gained from our data collection campaign. To achieve this, we take an *actigraphy* based approach towards sleep quality monitoring, where we classify the stage of each minute as *sleep* or *awake* period. Our approach is inspired by the classic light-weight actigraphy based method proposed in [40], which determines sleep-awake stage of a minute by taking into account body movement related information corresponding to the surrounding minutes. The activity sleep-awake scores determined by their technique have been shown to agree with EEG based sleep monitoring 94.46% of the time [40]. In our implementation, we adopt the following model from their work, which takes 4 previous minutes and 2 following minutes into account to classify stage of the current minute: $s_m = \rho \times (w_{-4}a_{-4} + w_{-3}a_{-3} + w_{-2}a_{-2} + w_{-1}a_{-1} + w_0a_0 + w_{+1}a_{+1} + w_{+2}a_{+2})$. where s_m is the average sleep-awake score for the current minute, ρ is a scaling factor, a_{-i}, a_0, a_{+i} are activity scores (normalized number of body movement events in each minute) for previous, current and following minutes, and w_{-i}, w_0, w_{+i} represent weights for the previous minutes, current minute and following minutes. If $s_m \leq 1$, the current minute's stage is classified as *sleep*, and if $s_m > 1$, the current minute's stage is classified as *awake*. In our implementation, we chose $\rho = 0.125, w_{-4} = 0.15, w_{-3} = 0.15, w_{-2} = 0.15, w_{-1} = 0.08, w_0 = 0.21, w_1 = 0.12, w_2 = 0.13$, as suggested by the authors of [40] for best results in their real-world deployments.

Figure 13 shows three different metrics of sleep determined for 3 users over a period of more than 13 consecutive

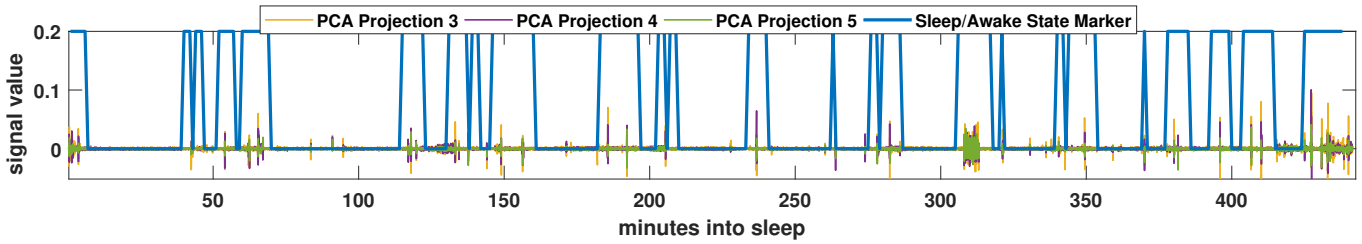

Fig. 12: Example showing Sleep/Awake classification for full night's sleep of a subject. Sleep efficiency was 62.1%.

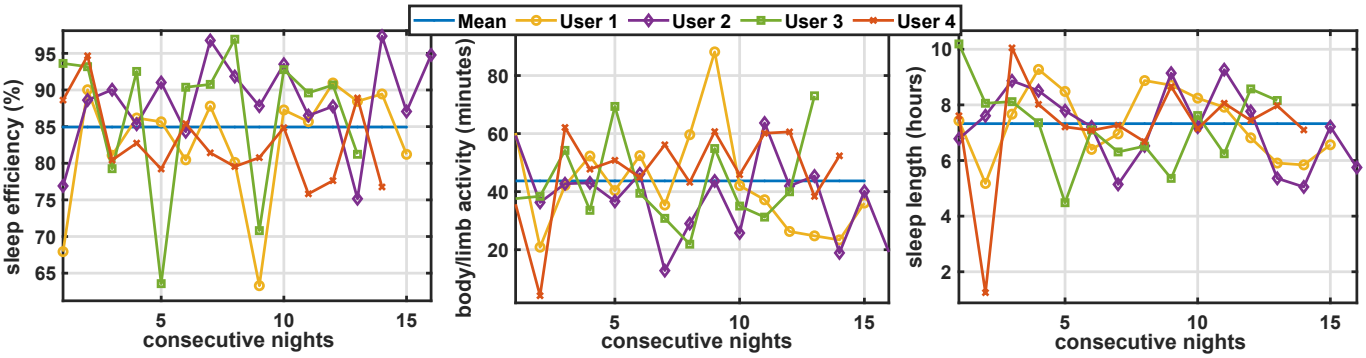

Fig. 13: Sleep efficiency and body motion corresponding to 4 users and throughout 13+ consecutive nights.

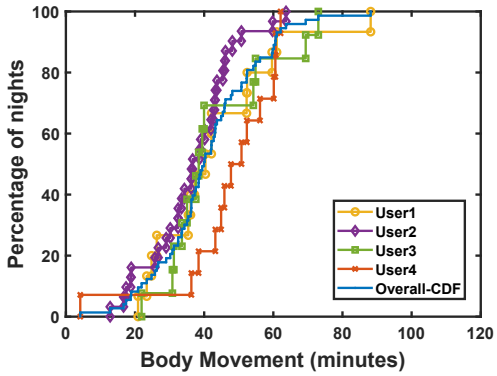

(a) Overall and per-user CDF for motion duration.

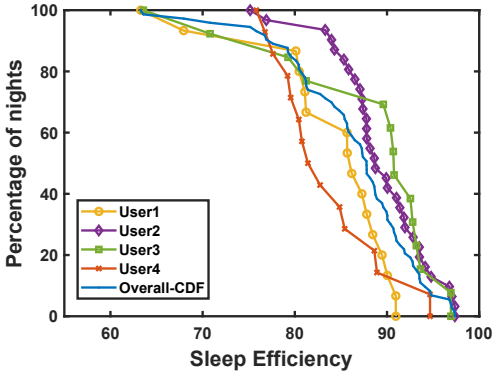

(b) Overall and per-user CCDF for sleep efficiency

Fig. 14: CDFs for motion duration and sleep efficiency.

days, namely *sleep efficiency*, *aggregate motion* (in minutes) during sleep and *sleep length*. Sleep efficiency for each night of sleep was calculated using on our actigraphy based sleep scoring approach, which is defined as the ratio of actual time spent in sleep stages to total time spent in bed (i.e. $T_{sleep}/(T_{sleep} + T_{awake})$). Figure 12 shows Sleep/Awake classification performance for full night's sleep of a subject, where sleep efficiency was determined to be 62.1%. As users manually started and ended each night's data collection using our software, the sleep lengths were easily determined according to those end points. We observe interesting insights for these long term sleep metrics. For instance, we can see that User 1 experienced a noticeably restless 9th night which resulted in poor sleep efficiency. User 4 only slept for 1.25 hours, but as he was awake for only 4.156 minutes during that time, his sleep efficiency reaches 95%.

In terms of aggregate body motion statistics over nights and across subjects, we measured a median of 40 minutes with the 95th percentile being under 80 minutes as illustrated in the blue CDF in figure 14(a). On an individual basis, and considering user 2 and user 4 for instance, their median body movements were 36 minutes and 47 minutes, respectively. This insight is corroborated when inspecting the complementary CDF's depicted in figure 14(b). Specifically, while both users 2 and 3 have a comparable maximum sleep efficiency of 96%, User 3's sleep efficiency was lower than 80% on 3 different nights. Moreover, User 2 has a worst efficiency of 75%, whereas User 3 has worst efficiency of 63%. For the aggregate dataset, the median user population sleep efficiency was around 87%. The average sleep duration among these 3 users during this consecutive testing period was 7.32 hours. Note that the recommended sleep for ages 18-64 years is 7-9 hours [33].

Limitations of WiFi signals based sleep vital signs monitoring. Our results show that WiFi based sleep monitoring can be significantly affected by changes in a user's sleep postures and activities of other house residents while the user is sleeping. The breath rate error can vary between 0.34 BPM to more than 5 BPM depending upon the time of night as a user's sleep posture and distance from the sleep monitor can change during sleep. Breath signal outages arise due to subjects rolling over in bed to a different position and/or sleep posture that makes it difficult to pick up the subjects' chest movements for a while. Tracking position and sleep posture using WiFi signals is a difficult problem to solve and addressing it requires a separate dedicated research study. Some recent works have proposed RFID tags based [41] and

Frequency Modulated Carrier Waves (FMCW) signals based [42] approaches to address this problem.

Extracting breath signal during other motions: When other motions occur in the vicinity of a sleeping user, they usually dwarf the changes introduced in WiFi signals by breathing. Even if non-breathing motions are small (e.g. head or arm movement), once the breath signals are entangled with signals related to other motions, it is extremely hard to extract the breath related signals. A similar problem is faced if we want to track breath of multiple people sleeping in a room simultaneously. Signal separation techniques such as Independent Component Analysis (ICA) can be tried. However, such techniques usually require strong assumptions. Specifically, in ICA, the goal is to recover the signal sources and the mixing matrix given only the observations, provided that the sources are independent, non-Gaussian, and combine linearly at the receiver end. In our opinion, these are very strong assumptions when using COTS WiFi devices (with many non-idealities, such as limited sensing capabilities, dynamic range, and aperture/spatial diversity, etc.) for sensing. Multi-person breath tracking using RF signals has been explored recently by researchers [26]. However, they use FMCW radar signals and hardware that are specialized for sensing. In [26], the spatial domain is shown to be able to resolve two adjacent motions and disentangle breathing signals from multiple users using a dedicated large aperture FMCW radar. With WiFi operating at a comparatively tiny fraction of bandwidth and much smaller antenna array, it may be difficult to achieve similar results. However, a dedicated research study is required before strong statements can be made.

Data collection. Although the data we collected is from a limited population sample, we collected it over a duration spanning several months i.e. results are stress-tested against significant time non-stationarity often referred to as "different days" experiments in general RF sensing literature. We feel that compared to the previous works, we have collected a good volume of data. Although our dataset is not exhaustive when measured on an industrial scale, the volume is representative and sufficient for highlighting some of the trends and difficulties of re-purposing COTS WiFi for sleep monitoring. Orchestrating a study involving a large cohort of users is outside the scope of this work.

Sleep stage classification. A more ambitious learning task pertaining to sleep monitoring is sleep stage classification [43]. It has been shown in prior art using custom radar signalling that wireless sleep 4-stage classification can be achieved through a domain adaptation approach paired with ground truth from medical-grade devices [44]. The Xethru radar we use in our comparative study does not provide sleep stage classification information. Nonetheless, we have demonstrated in this paper the elements of sleep monitoring needed for such classification; namely, breathing and motion estimation. To investigate the potential extension of this work towards 4-stage sleep classification, we have conducted a limited pilot study using sleep versus awake classification information obtained from a commercial ResMed S+ sleep monitoring device [45]. For demonstration purposes, we apply a simple feature engineering approach using statistical features derived from our respiration estimate. Figure 15 depicts a snapshot of such classification over an entire night. From close inspection, it is evident that the results of this relatively simple approach turn out to be quite similar to that of ResMed S+. Therefore, we believe that advanced sleep-stage classification is possible by using both body movement and respiration based vital signs obtained from our system. However, testing the accuracy of a WiFi based solution compared to the Polysomnography (PSG) gold-standard would require a dedicated study and significant data collection effort. We leave expanding this research strand for future work.

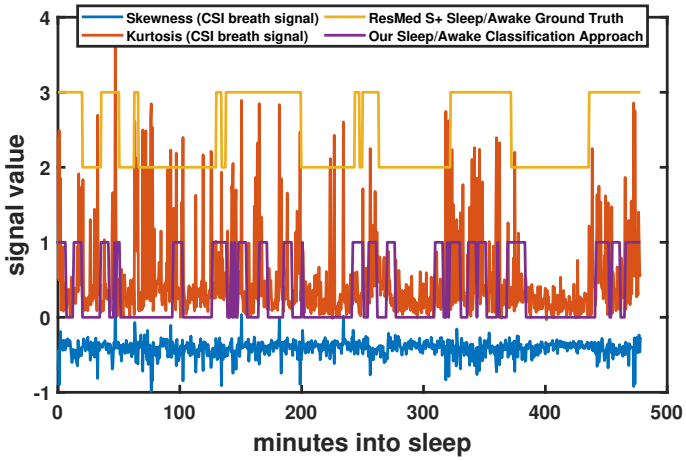

Fig. 15: Two-stage (asleep versus awake) crude classification using simple feature engineering approach and as compared to classification from a commercial ResMed S+ device.

WiFi vs Bluetooth for sleep monitoring. Bluetooth devices usually have higher energy constraints compared to the WiFi devices of everyday use. For example, WiFi devices are usually either regularly charged by the users (e.g. smartwatches, smartphones, laptops, etc.) or are continuously plugged in (e.g. WiFi routers). Therefore, establishing a dedicated connection between any two WiFi devices for long term sensing purposes makes for a better use case. Also, Bluetooth received signal strength (RSSI) information is much coarser grained compared to the WiFi CSI information, making it difficult to extract any useful breathing information. Moreover, Bluetooth devices usually have just one antenna so we cannot utilize beamforming to improve the good quality of breath signals. However, it may be possible to fuse the lower-level PHY information of Bluetooth devices (e.g. RSSI) over multiple frequencies during the frequency hopping process to improve the fidelity of breath signals. Although a dedicated study on Bluetooth based sleep monitoring is out of the scope of our current work, yet we feel that this can be an interesting topic for future research.

Modifying WiFi to improve sensing. The goal of this work is to leverage the existing WiFi hardware and protocols for sleep monitoring, without any modification. However, we believe that adding dedicated "radar-like" capabilities to WiFi systems can significantly improve their sensing capability. Researchers are already working on developing such specialized hardware for sleep monitoring applications [25], [26], [42], however, their system does not have any

WiFi like communication capability yet. Developing WiFi systems that can jointly optimize communication and sensing signaling, which can in turn be adapted according to the requirements of different sensing applications, is an open problem and a very interesting research direction.

6 Related Work

6.1 Respiration, Body Movements and Sleep

Previous works have shown that breathing and body movements during sleep are closely related to sleep quality in humans [33], [2], [46]. These studies show that respiratory dynamics vary over sleep stages, which means that respiratory activity can be used to separate sleep stages [33]. For example, Dafna *et al.* evaluated whole night sleep based on sleep-awake classification using audio recordings of breathing sounds [46]. They captured and quantified variations in breathing features such as periodicity and consistency, and showed that these features contribute to distinguishing between sleep and wake epochs.

6.2 Sleep Monitoring Technologies

Several sleep monitoring techniques have been proposed in the past which use different sensing modalities, such as in-ear [47], inertial sensors (Actigraphy) [48], [1], [2], [3], [4], [5], [6], [7], EEG [8], Audio [10], [11], [12], Video [13], [14], Bed sensors (*e.g.* Ballistocardiography (BCG), pressure and/or motion sensors based techniques) [15], [16], [17], [18], [19], [20] and RF sensing based techniques (*e.g.* mmWave, Frequency Modulated Continuous Wave (FMCW) radar, Pulse-Doppler radar, RFID and WiFi based techniques) [27], [28], [21], [22], [23], [24], [25], [26]. For brevity, we will only discuss some of the closely related recent works on contactless sleep monitoring, which include some sound, radar and WiFi CSI based techniques.

Lullaby [49] tracks various environmental factors, sound, light, temperature, and motion that help users assess the quality of their sleep environments. iSleep [10] uses the built-in microphone of the smartphone to detect the events that are closely related to sleep quality, including body movement, couch and snore, and infers quantitative measures of sleep quality. Sleep Hunter [50] uses actigraphy and acoustic events to predict sleep stage transitions by smartphone. Toss-N-Turn [51] uses features such as sound amplitude, acceleration, light intensity, screen proximity, battery and screen states, etc. to track a subject's sleep quality. However, Audio based techniques are privacy invasive, and therefore, often avoided as sleep is a private activity.

RF sensing based techniques are by far the least intrusive methods for monitoring sleep, both in terms of privacy and convenience of use. DoppleSleep [21] is another unobtrusive sleep sensing system which uses short-range Doppler radar to perform sleep stage classification (Sleep vs. Wake and REM vs. Non-REM). Vital-radio [25] develop an FMCW based system which is shown to accurately track a person's breathing and heart rate without body contact, from distances up to 8 meters. Based on the same system, [44] proposes a deep learning architecture to perform 4-stage sleep stage classification. More recently, authors of [26] proposed algorithms to achieve multi-person identification and breath monitoring based on the same FMCW hardware. Although the aforementioned radar based techniques do fairly well in terms of monitoring vital signs during sleep. However, they require dedicated hardware and spectrum, adding cost, scalability (e.g., when multiple such radars are co-located), and/or RF regulation hurdles. These factors prevent their large-scale and long-term deployment. WiFi signals based sensing has recently emerged an approach to low-cost and easily adoptable long-term sleep monitoring, as the widespread use of WiFi capable devices (*e.g.* smart-home assistants, smart-phones, etc.) has made WiFi signals the most ubiquitous form of sensing in homes requiring no additional hardware costs. Multiple WiFi CSI based schemes have been proposed for tracking vital signs during sleep [29], [23], [22], [30], [31]. The key limitation of the existing works is that they have only been evaluated with short-duration mock sleep experiments in very controlled settings. This makes the applicability of their techniques and findings quite limited in practical sleep monitoring scenarios. For example, the techniques proposed in existing works have been designed based on controlled experiments often performed on the same subject, where they require the subject to lie down in between and/or very close to both transmitter (TX) and the receiver (RX) to ensure line-of-sight (LOS) scenarios. Their techniques rely on trial-and-error based positioning of WiFi transceivers and signal processing methods to track vital signs, which often leads to high dependency on multiple, environment-dependent parameters that are difficult to tune in real world. Such techniques may be suitable for controlled short-duration lab experiments. However, their suitability cannot be generalized to different individuals, environments, positioning of WiFi transceivers, LOS/NLOS situations, and to natural in-home full-night sleeping scenarios.

7 Conclusions

In this paper, we make two key contributions. First, we characterize the relationship between WiFi signal components (i.e. multipath and signal subspace) and human vital signs (i.e. respiration and body motions). Grounded in this characterization, we propose two methods: 1) a respiration tracking technique that models the peak dynamics observed in the time-varying signal subspaces and 2) a body-motion tracking technique built with a multi-dimensional clustering of evolving signal subspaces. Second, we extensively evaluate our proposed methods through real-world full-night sleep experiments conducted in 5 different apartments, where we collected more than $>$550 hours (80 nights) of data from 5 users. Our results demonstrate that the proposed techniques were able to track respiration rate with an average error of $<$1.19 breaths per minute (BPM). However, the breath rate error varied between 0.34 BPM to more than 5 BPM depending upon the time of night as a user's sleep posture and distance from the sleep monitor can change during sleep. Co-located activities of other house residents also affect WiFi based vital signs monitoring. We conclude that WiFi based sleep monitors can be robust and accurate enough for in-home use to gain insights into overall breath and motion trends. However, the accuracy may not be enough for medical-grade sleep assessments.

REFERENCES

[1] Avi Sadeh, Peter J Hauri, Daniel F Kripke, and Peretz Lavie. The role of actigraphy in the evaluation of sleep disorders. *Sleep*, 1995.

[2] Avi Sadeh and Christine Acebo. The role of actigraphy in sleep medicine. *Sleep medicine reviews*, 2002.

[3] Sonia Ancoli-Israel, Roger Cole, Cathy Alessi, Mark Chambers, William Moorcroft, and Charles P Pollak. The role of actigraphy in the study of sleep and circadian rhythms. *Sleep*, 2003.

[4] Xi Long, Pedro Fonseca, Jérôme Foussier, Reinder Haakma, and Ronald M Aarts. Sleep and wake classification with actigraphy and respiratory effort using dynamic warping. *IEEE journal of biomedical and health informatics*, 2014.

[5] Fitbit. Fitbit. https://www.fitbit.com/, July 2018.

[6] Xiaomi. Xiaomi mi band 3. https://www.mi.com/en/miband/, July 2018.

[7] O. Oura ring. https://ouraring.com/, July 2018.

[8] Gibson Research Corporation. Zeo sleep manager pro. https://uk.pcmag.com/zeo-sleep-manager-pro/5064/review/zeo-sleep-manager-pro, December 2012.

[9] Eun Kyoung Choe, Julie A Kientz, Sajanee Halko, Amanda Fonville, Dawn Sakaguchi, and Nathaniel F Watson. Opportunities for computing to support healthy sleep behavior. In *ACM CHI*, 2010.

[10] Tian Hao, Guoliang Xing, and Gang Zhou. isleep: unobtrusive sleep quality monitoring using smartphones. In *Proc. of ACM Sensys*, 2013.

[11] Dirk Pevernagie, Ronald M Aarts, and Micheline De Meyer. The acoustics of snoring. *Sleep medicine reviews*, 2010.

[12] GR De Bruijne, PCW Sommen, and RM Aarts. Detection of epileptic seizures through audio classification. In *4th European conference of the Int. Federation for Medical and Biological Engineering*. Springer, 2009.

[13] Adrienne Heinrich, Frank van Heesch, Bhargava Puvvula, and Mukul Rocque. Video based actigraphy and breathing monitoring from the bedside table of shared beds. *Journal of Ambient Intelligence and Humanized Computing*, 2015.

[14] Ming-Zher Poh, Daniel J McDuff, and Rosalind W Picard. Advancements in noncontact, multiparameter physiological measurements using a webcam. *IEEE Transactions on Biomedical Engineering*, 2011.

[15] Matteo Migliorini, Anna M Bianchi, Domenico Nisticò, Juha Kortelainen, Edgar Arce-Santana, Sergio Cerutti, and Martin O Mendez. Automatic sleep staging based on ballistocardiographic signals recorded through bed sensors. In *IEEE EMBC*, 2010.

[16] Joonas Paalasmaa, Mikko Waris, Hannu Toivonen, Lasse Leppäkorpi, and Markku Partinen. Unobtrusive online monitoring of sleep at home. In *IEEE EMBC*, 2012.

[17] Juha M Kortelainen, Martin O Mendez, Anna Maria Bianchi, Matteo Matteucci, and Sergio Cerutti. Sleep staging based on signals acquired through bed sensor. *IEEE Transactions on Information Technology in Biomedicine*, 2010.

[18] Wenxi Chen, Xin Zhu, Tetsu Nemoto, Yumi Kanemitsu, Keiichiro Kitamura, and Ken-ichi Yamakoshi. Unconstrained detection of respiration rhythm and pulse rate with one under-pillow sensor during sleep. *Medical and Biological Engineering and Computing*, 2005.

[19] Byung Hun Choi, Gih Sung Chung, Jin-Seong Lee, Do-Un Jeong, and Kwang Suk Park. Slow-wave sleep estimation on a load-cell-installed bed: a non-constrained method. *Physiological measurement*, 2009.

[20] Withings. Withings sleep tracking mat. https://www.withings.com/us/en/sleep, 2018.

[21] Tauhidur Rahman, Alexander T Adams, Ruth Vinisha Ravichandran, Mi Zhang, Shwetak N Patel, Julie A Kientz, and Tanzeem Choudhury. Dopplesleep: A contactless unobtrusive sleep sensing system using short-range doppler radar. In *Proc. of ACM Ubicomp*, 2015.

[22] Xuefeng Liu, Jiannong Cao, Shaojie Tang, and Jiaqi Wen. Wi-sleep: Contactless sleep monitoring via wifi signals. In *IEEE RTSS*, 2014.

[23] Jian Liu, Yan Wang, Yingying Chen, Jie Yang, Xu Chen, and Jerry Cheng. Tracking vital signs during sleep leveraging off-the-shelf wifi. In *Proc. of ACM MobiHoc*, 2015.

[24] Zhicheng Yang, Parth H Pathak, Yunze Zeng, Xixi Liran, and Prasant Mohapatra. Monitoring vital signs using millimeter wave. In *Proc. of ACM MobiHoc*, 2016.

[25] Fadel Adib, Hongzi Mao, Zachary Kabelac, Dina Katabi, and Robert C Miller. Smart homes that monitor breathing and heart rate. In *Proc. of ACM CHI*, 2015.

[26] Shichao Yue, Hao He, Hao Wang, Hariharan Rahul, and Dina Katabi. Extracting multi-person respiration from entangled rf signals. *ACM IMWUT*, 2018.

[27] Cecilia Occhiuzzi and Gaetano Marrocco. The rfid technology for neurosciences: feasibility of limbs' monitoring in sleep diseases. *IEEE Transactions on Information Technology in Biomedicine*, 2010.

[28] Cecilia Occhiuzzi, Carmen Vallese, Sara Amendola, Sabina Manzari, and Gaetano Marrocco. Night-care: A passive rfid system for remote monitoring and control of overnight living environment. *Elsevier Procedia Computer Science*, 2014.

[29] Peter Hillyard, Anh Luong, Alemayehu Solomon Abrar, Neal Patwari, Krishna Sundar, Robert Farney, Jason Burch, Christina Porucznik, and Sarah Hatch Pollard. Experience: Cross-technology radio respiratory monitoring performance study. In *ACM MOBICOM*, 2018.

[30] Hao Wang, Daqing Zhang, Junyi Ma, Yasha Wang, Yuxiang Wang, Dan Wu, Tao Gu, and Bing Xie. Human respiration detection with commodity wifi devices: do user location and body orientation matter? In *Proc. of ACM Ubicomp*, 2016.

[31] Fusang Zhang, Daqing Zhang, Jie Xiong, Hao Wang, Kai Niu, Beihong Jin, and Yuxiang Wang. From fresnel diffraction model to fine-grained human respiration sensing with commodity wi-fi devices. *ACM IMWUT*, 2018.

[32] Daniel Halperin, Wenjun Hu, Anmol Sheth, and David Wetherall. Tool release: gathering 802.11 n traces with channel state information. *ACM SIGCOMM Computer Communication Review*, 2011.

[33] Xi Long. On the analysis and classification of sleep stages from cardiorespiratory activity. *SLEEP-WAKE*, 2015.

[34] M. Alloulah, A. Isopoussu, C. Min, and F. Kawsar. On Tracking the Physicality of Wi-Fi: A Subspace Approach. *IEEE Access*, 7:19965–19978, 2019.

[35] M. Moshtaghi and et. al. Incremental elliptical boundary estimation for anomaly detection in wireless sensor networks. In *IEEE ICDM*, 2011.

[36] Xethru. Respiration sensor x4m200. https://www.xethru.com/x4m200-respiration-sensor.html, 2018.

[37] SolidRun. Hummingboard. https://www.solid-run.com/nxp-family/hummingboard/, 2018.

[38] Xethru. Xethru vs. polysomnography (psg) comparative study. https://www.xethru.com/community/resources/categories/white-papers.6/.

[39] Ali Abdi, Kyle Wills, H Allen Barger, M-S Alouini, and Mostafa Kaveh. Comparison of the level crossing rate and average fade duration of rayleigh, rice and nakagami fading models with mobile channel data. In *Vehicular Technology Conf. , 2000. IEEE-VTS Fall VTC 2000. 52nd*, volume 4, pages 1850–1857. IEEE, 2000.

[40] John B Webster, Daniel F Kripke, Sam Messin, Daniel J Mullaney, and Grant Wyborney. An activity-based sleep monitor system for ambulatory use. *Sleep*, 1982.

[41] Jia Liu, Xingyu Chen, Shigang Chen, Xiulong Liu, Yanyan Wang, and Lijun Chen. Tagsheet: Sleeping posture recognition with an unobtrusive passive tag matrix. In *IEEE INFOCOM*, 2019.

[42] Shichao Yue, Yuzhe Yang, Hao Wang, Hariharan Rahul, and Dina Katabi. Bodycompass: Monitoring sleep posture with wireless signals. *ACM IMWUT*, 2020.

[43] Richard B Berry, Rita Brooks, Charlene E Gamaldo, Susan M Harding, CL Marcus, BV Vaughn, et al. The aasm manual for the scoring of sleep and associated events. *Rules, Terminology and Technical Specifications, Darien, Illinois, American Academy of Sleep Medicine*, 2012.

[44] Mingmin Zhao, Shichao Yue, Dina Katabi, Tommi S Jaakkola, and Matt T Bianchi. Learning sleep stages from radio signals: a conditional adversarial architecture. In *IEEE ICML*, 2017.

[45] RedMed. S+ sleep sensor. https://www.resmed.com/us/en/consumer/s-plus.html, 2018.

[46] Eliran Dafna, Ariel Tarasiuk, and Yaniv Zigel. Sleep-wake evaluation from whole-night non-contact audio recordings of breathing sounds. *PloS one*, 2015.

[47] Anh Nguyen, Raghda Alqurashi, Zohreh Raghebi, Farnoush Banaei-Kashani, Ann C Halbower, and Tam Vu. Libs: A lightweight and inexpensive in-ear sensing system for automatic whole-night sleep stage monitoring. *GetMobile: Mobile Computing and Communications*, 2017.

[48] Xiao Sun, Li Qiu, Yibo Wu, Yeming Tang, and Guohong Cao. Sleepmonitor: Monitoring respiratory rate and body position during sleep using smartwatch. *Proc. of ACM IMWUT*, 2017.
[49] Matthew Kay, Eun Kyoung Choe, Jesse Shepherd, Benjamin Greenstein, Nathaniel Watson, Sunny Consolvo, and Julie A Kientz. Lullaby: a capture & access system for understanding the sleep environment. In *Proc. of ACM Ubicomp*, 2012.
[50] Weixi Gu, Zheng Yang, Longfei Shangguan, Wei Sun, Kun Jin, and Yunhao Liu. Intelligent sleep stage mining service with smartphones. In *Proc. of ACM Ubicomp*, 2014.
[51] Jun-Ki Min, Afsaneh Doryab, Jason Wiese, Shahriyar Amini, John Zimmerman, and Jason I Hong. Toss'n'turn: smartphone as sleep and sleep quality detector. In *Proc. of ACM CHI*, 2014.

Kamran Ali graduated with a Ph.D. in Computer Science and Engineering from Michigan State University, USA, in 2019. He is now with General Motors R&D. He received his B.S. degree in Electrical Engineering and Computer Sciences in 2013, from School of Science and Engineering (SSE) of Lahore University of Management Sciences (LUMS), Pakistan. He has worked with Hewlett Packard Labs, NEC Laboratories, Nokia Bell Labs, and Microsoft's Applied Sciences Group during his PhD. His research interests lie in the areas of Sensing Systems, Applied Machine Learning, Signal Processing, Wireless Communications, RF Sensing, Mobile Computing, and Internet of Things.

Mohammed Alloulah is with Nokia Bell Labs, USA. Mo obtained a PhD from Lancaster University, UK, jointly funded by Research Councils UK through a Dorothy Hodgkin postgraduate award and by a Microsoft Research Cambridge Scholarship. Mo has 14+ years experience in wireless & chips with silicon deployed in the field. Mo has led R&D and delivered systems in multiple industrial settings in areas spanning signal processing, ultra-low power medical wearables, and automotive radar. Recently, Mo has been leading projects in indoor wireless sensing, ultra-low power machine learning, and 6G networks. Outside work, Mo is a keen runner and a part-time cyclist.

Alex X. Liu received his Ph.D. degree in Computer Science from The University of Texas at Austin in 2006, and is an honorary professor of Qilu University of Technology. Before that, he was a Professor in the Department of Computer Science and Engineering at Michigan State University (MSU). He received the IEEE & IFIP William C. Carter Award in 2004, a National Science Foundation CAREER award in 2009, the MSU Withrow Distinguished Scholar (Junior) Award in 2011, and the MSU Withrow Distinguished Scholar (Senior) Award in 2019. He has served as an Editor for IEEE/ACM Transactions on Networking and an Area Editor for Computer Communications. He is currently an Associate Editor for IEEE Transactions on Dependable and Secure Computing and IEEE Transactions on Mobile Computing. He has served as the TPC Co-Chair for ICNP 2014 and IFIP Networking 2019. He received Best Paper Awards from SECON-2018, ICNP-2012, SRDS-2012, and LISA-2010. His research interests focus on networking, security, and privacy. He is an IEEE Fellow and an ACM Distinguished Scientist.

Fahim Kawsar leads the Internet of Things research at Bell Labs and holds a Design United Professorship at TU Delft. His current research explores novel algorithms and system design techniques to build transformative multi-sensory systems for disruptive mobile, wearable and IoT services. He borrows tenets from Social Psychology, learns from Behavioural Economics and applies Computer Science methods to drive his research. He is a frequent keynote, panel and tutorial speaker, hold 15+ patents, organised and chaired numerous conferences, (co-)authored 100+ publications and has had projects commissioned. He is a former Microsoft Research Fellow and has worked before at Nokia Research, and Lancaster University. Fahim obtained his MSc and PhD degrees both in Computer Science from Waseda University, Japan, respectively in 2006 and 2009.